Branching Features of Amylopectins and Glycogen Determined by Asymmetrical Flow Field Flow Fractionation Coupled with Multiangle Laser Light Scattering

Agnès Rolland-Sabaté,* Paul Colonna, Maria Guadalupe Mendez-Montealvo,† and Véronique Planchot

Biopolymères Interactions Assemblages, INRA, F-44300 Nantes Cedex 03, France

Received January 8, 2007; Revised Manuscript Received April 25, 2007

The aim of this work was to characterize starch polysaccharides using asymmetrical flow field flow fractionation coupled with multiangle laser light scattering. Amylopectins from eight different botanical sources and rabbit liver glycogen were studied. Amylopectins and glycogen were completely solubilized and analyzed, and high mass recoveries were achieved (81.7−100.0%). Amylopectin $\bar{M}_{w,}$ $\bar{R}_G$, and the hydrodynamic coefficient ν_G (the slope of the log−log plot of R_{Gi} vs M_i) were within the ranges 1.05−3.18 × 10^8 g mol^{-1}, 163−229 nm, 0.37−0.49, respectively. The data were also considered in terms of structural parameters. The results were analyzed by comparison with the theory of hyperbranched polymers (Flory, P. J. *Principles of Polymer Chemistry*; Cornell University Press: Ithaca, NY, 1953; Burchard, W. *Macromolecules*, **1977**, *10*, 919−927). This theory, based upon the ABC model, has been shown to underestimate the branching degrees of amylopectins. However, quantitative agreement with the data in the literature was found for amylopectins when using the ABC model modified by the introduction of a multiplying factor, determined from previously described amylopectin structures in terms of the number of branching point calculations.

Introduction

Starch is the principal storage carbohydrate polysaccharide in higher plants, being the end product of photosynthesis. Its main uses are foods and feeds for energy but also for its functional properties. Starch is used as a thickening, stabilizing, or gelling agent in food products. These properties are determined by macromolecular characteristics and the conformation in solution of the polymers used. Although food safety is now stringently controlled at the European level, the control of qualitative properties is still a bottleneck for both users and consumers. The exploration of biological variability is reinforced by an opportunity to create new genotypes using results from genomic studies. In this context, the characterization of starch macromolecules is of considerable importance to their assessment.

Starch consists of a mixture of two α-glucans built mainly upon α-(1,4) linkages. Amylose is essentially linear, whereas amylopectin has a branched structure with 5−6% α-(1,6) linkages.[1] They also have different weight average molar masses, radii of gyration, and hydrodynamic radii: $\bar{M}_w \approx 10^5-10^6$ g mol^{-1}, $\bar{R}_G \approx 10-60$ nm, and $\bar{R}_H \approx 10-30$ nm for amylose and $\bar{M}_w \approx 10^6-10^8$ g mol^{-1} and $\bar{R}_G \sim \bar{R}_H \approx 200$ nm for amylopectin.[2] These polysaccharides have been characterized quantitatively by high-performance size-exclusion chromatography (HPSEC) combined with multiangle laser light scattering (MALLS).[3,4] The limitation of HPSEC columns is their low exclusion limit regarding amylopectin size. The fractionation of amylopectin in silica gel HPSEC columns with low porosity such as TSK gel SW_{XL} G2000 from TosoHaas (Stuttgart, Germany) results from the combined effect of hydrodynamic chromatography (HDC) occurring in the void volume on the one hand and size-exclusion chromatography (SEC) on the other hand.[5] Because of this, further improvements are necessary to obtain the entire distribution of amylopectin to achieve its complete structural characterization. Flow field flow fractionation (FFFF) is an almost universal technique, the selectivity of which is based on the diffusion coefficient.[6] The fractionation range covers a broad band of molecular or particle sizes from ∼50 nm (depending on the membrane cutoff) up to 50 μm. FFFF is a chromatographic method that does not involve a stationary phase. Separation takes place in a laminar flow and is caused by a field force that is represented by a flow perpendicular to the carrier flow (crossflow). Asymmetrical FFFF (AFFFF) is a variant of FFFF that only uses one permeable wall as the accumulation wall (a frit covered by an ultrafiltration membrane).[6−8] AFFFF experiments are based on three successive phases: (i) setting of the samples by injection/relaxation/focusing, (ii) elution, and (iii) backflushing. During the first phase, the flow is directed to enter the channel via the inlet, the only outlet being through the membrane. The sample is introduced into the channel during this phase and focused at the position in the channel determined by the counteracting flows, where the axial velocity is zero. Sample components move to equilibrium height over the membrane. The next phase is elution, where the flow enters the channel from the inlet and leaves both through the membrane (creating the crossflow) and through the channel outlet. The carrier flow is laminar into the channel, so the transportation speed of the sample is correlated to its distance from the membrane wall. The interplay between field-induced migration toward this membrane and Brownian motion away from the wall leads to an exponential decrease with increasing

* Author to whom correspondence should be addressed. Phone: +33 (0) 240 67 51 48. Fax: +33 (0) 240 67 51 67. E-mail: sabate@nantes.inra.fr.

† Present address: Centro Dessarollo de Productos Bioticos, Carr. Yautepec-Jotula Km 8.5 Col. Son Isidro, 72630 Yautepec Morelos, Mexico.

10.1021/bm070024z CCC: $37.00
Published on Web 07/24/2007

distance from the membrane. This corresponds to the normal mode operation under which small particles are eluted first. According to the AFFFF theory,[8−11] the elution time in normal mode t_{ri} (or the retention ratio $R = t_0/t_{ri}$, where t_0 is the void time) is related to the translational coefficient of diffusion D_i of the *i*st slice

$$R = t_0/t_{ri} \approx 6D_iV_0/F_cw^2 \quad (1)$$

where F_c is the crossflow rate, w the channel thickness, and V_0 the void volume. For $R \leq 0.44$ the error in eq 1 is less than 10%.[10] For polydispersed samples, working with a crossflow gradient would enable better fractionation of the entire sample than with a constant crossflow. For a linear regression of crossflow with time, t_{ri} could be expressed as[11]

$$t_{ri} = t_{start} + (t_{end} - t_{start})\{1 - \exp[-((t_0\, w^2F_c(\text{start})/6D_iV_0) - t_{start}))/(t_{end} - t_{start})]\} \quad (2)$$

where t_{start} is the time corresponding to the start of the gradient and t_{end} is the time corresponding to the end of the gradient, $t_{end} > t_{ri} > t_{start}$.

FFFF has been used to investigate the fractionation of compounds with a high molecular size,[12] such as gum Arabic,[13] ethylhydroxyethyl cellulose,[14] native starches[15,16] and amylopectins,[17] and chemically modified starches.[18−20] Roger[15] and You[16] employed symmetrical FFFF devices. However, You's procedure[16] generated very low elution recovery (50%) for barley starch with zero amylose content. Using an AFFFF system presents an advantage when compared with symmetrical FFFF devices:[15] The injection procedure enables better separation because the sample forms a narrow band at the beginning of the measurement. Van Bruijnsvoort[17] used an AFFFF device with a small channel thickness (130 μm) that produced the hyperlayer fractionation of amylopectins in addition to an overloading effect, so molar mass values presented high standard deviations. Studies concerning cationic amylopectins[19,20] using an AFFFF device with a standard channel thickness (250 μm) revealed relatively good fractionation of these compounds, which presented average molar masses that were 10 times lower than those of corresponding native amylopectins. A few programmed field separations of polymers have been published,[14,21] and they open interesting perspectives for polydispersed samples such as amylopectins. However, the two major drawbacks mentioned in most publications should also be pointed out: the state of solubilization and incomplete recovery of the injected sample. Complete solubilization of the starch sample in the eluent without macromolecular degradation is a prerequisite for determining the molecular weight distributions of amylose and amylopectin and their average molar masses using any technique. In most cases, elution recovery rates are not mentioned in publications. Moreover, some authors reported 84−100% recovery for maize starches,[15] 92−95% recovery for jet-cooked cationic amylopectins,[20] and 60−89% recovery for hydroxyethyl waxy maize starches,[18] the two latter cases corresponding to macromolecules with lower molar masses than neutral native amylopectins.

Yu and Rollings[22] approached the amylopectin branching parameter (or shrinking factor) g_M, defined by Zimm and Stockmayer[23] as the ratio between the square of the radius of gyration of the branched polymer and the square of the radius of gyration of the corresponding linear polymer for the same molar mass. To achieve this goal, they used HPSEC separation coupled with low-angle laser light-scattering detection on native amylopectins, and the relationship between g_v (which is the ratio between the molar mass of the linear and branched polymer at the same elution volume) and g_M. Later, branching characteristics were evaluated for nonfractionated degraded potato starches[24,25] and SEC-fractionated native starches[26] using light scattering for g_M determination and the theory of hyperbranched structures for branching evaluation. These studies dealt with total starch, including amylose populations without or with incomplete fractionation of the samples.

A new approach for studying branching features is to gain insight into the characterization of branched polymers such as amylopectin. The basic organization of amylopectin branching is described in terms of outer chains (A), which are glycosidically linked to an inner chain (B), defined as chains bearing other chains as branches.[1] Amylopectin is constituted by short chains (S) including external (A) and internal (B) chains (degree of polymerization (DPs) of 15−20), by long B chains (L) (DP of 40−45), and some very long chains B (DP higher than 60). Short chains are organized in clusters. The cluster model structure proposed by French[27] and Robin[28] is now largely accepted. According to this, amylopectin is made of clusters that bring together all short chains, the clusters being linked by long chains with an average DP of 20−23 units between two successive clusters. The main difference as a function of botanical origin is the ratio between the short and long chains (S/L). This ratio is ~5 for tubers and 8−10 for cereal starches.[29] Cluster regions where all branching points are located are defined as branching zone clusters (BZCs).[30] Cluster geometry (the distance between two α-(1,6) linkages in the BZC and the number and length of linear chains inside the cluster) determines the development of crystallinity inside the starch granule.[30]

Different methods have been described to study amylopectin branching characteristics; most of them are based upon selective enzymatic hydrolysis of the macromolecule followed by characterization of the hydrolyzed fragments. Bertoft accessed the structural characteristics of amylopectin through a sequence of selective enzymatic hydrolyses followed by characterization of the fragments at different stages by SEC analysis.[31−34] The problem of branching concentration was approached using limited α-amylolysis to isolate clusters by the preferential hydrolysis of long B chains. A cluster was then an arrangement of branch points sufficiently close together to hinder α-amylase digestion of the connecting segments.[31,32,34] The intermediate dextrins were isolated and successively treated with phosphorylase and β-amylase to produce Φ,β-limit dextrins in which the external chains were reduced to maltosyl and glucosyl stubs.[31,33] More recently, a group of additional structural parameters were developed by Yao[35] taking account of the Hizukuri approach[36] and also working with the chain length (CL) distribution and relationships between branch points[33,37] to describe the branch density and branching pattern of amylopectin. Branch density was calculated from the average chain length ($\overline{CL}$) of amylopectin, and branching patterns were expressed in terms of the average number of branches per cluster, the modal cluster repeat distance, and the modal distance between adjacent branch points in the cluster. During that work, HPSEC was used to study debranched amylopectin and debranched β-limit dextrin to access the structural features of amylopectins.[35] A recent methodology was also developed to interpret the molecular weight distributions of debranched amylopectins obtained by fluorophore-assisted capillary electrophoresis (FACE).[38] In this methodology, a simple model for polymer synthesis was used. It was considered that the only events occurring are random chain growth and stoppage (these

processes are not chain-length-specific), so the number of chains with a degree of polymerization N, $P(N)$ is linear in ln $P(N)$ with a negative slope giving the ratio of the stoppage and growth rates. The plot of ln $P(N)$ versus N could be divided into characteristic regions corresponding to different growth stages of the amylopectin molecule. These regions could be assigned to specific enzymatic processes in starch synthesis, including determination of the ranges of the degrees of polymerization that are subjected to random and nonrandom processes. All of these experimental approaches are long and tedious and rather unsuited to the characterization of a large series of samples generated by postgenomic research.

Branching degree could also be determined by NMR analysis.[39] However, this method only produces an average value for the branching degree because there is no fractionation prior to NMR measurements. The aim of the present study was thus the complete structural characterization of native amylopectins, including their branching features, using a size fractionation technique. To achieve this, AFFFF separation in combination with MALLS and differential refractive index (DRI) techniques and data analysis using polymer science theories (ABC three-functional polycondensation model,[40] Zimm and Stockmayer theory[23]) were used. The structural properties of eight amylopectins and starches and rabbit liver glycogen were analyzed. Glycogen is an α-glucan built mainly upon α-(1,4) linkages that has a randomly branched structure with 8.0% α-(1,6) linkages.[41] It was used as a reference because of its highly dense branched structure.[41,42] This method, which takes 2−3 h, would enable the characterization of native amylopectins while avoiding lengthy and successive degradation steps.

Experimental Section

Materials. Starches containing amylopectin only were used: waxy maize starch (Roquette Frères, Lestrem, France), waxy rice starch (Remy Industries, Leuven-Wijgmaal, Belgium), waxy barley starch (5.4% amylose content) (Primalco Ltd., Finland), waxy wheat (Limagrain, Chappes, France), and amylose free (amf) potato starch (Lyckeby Stärkelsen Food & Fiber AB, Kristianstad, Netherlands). Manioc, normal maize, and smooth pea amylopectins were obtained after the thymol complexing of corresponding starches. Rabbit liver glycogen was obtained from Fluka (Saint Quentin Fallavier, France). Pullulan (P50) was purchased from Showa Denko K.K. (Tokyo, Japan). Monodispersed bovine serum albumin (BSA) was purchased from Sigma Chemical Company (St. Louis, MO). The water used was produced using a Milli-RQ-6-plus and Milli-Q-Plus purification system (Millipore, Bedford, MA).

Sample Preparation. Rabbit liver glycogen, pullulan, and BSA were directly solubilized in water containing 0.2 g L^{-1} sodium azide at room temperature. Prior to injection into the AFFFF-MALLS system, they were filtered through 0.45 μm Durapore membranes (Waters, Bedford, MA). As previously described,[4] starches were dimethylsulfoxide-pretreated, dried, and solubilized by microwave heating under pressure. Amylopectins were directly solubilized by microwave heating under pressure. Each sample suspension in water at a concentration of 0.5 g L^{-1} was heated for 40 s (maximal internal temperature reached, 152 °C) at 900 W. Amylopectin and starch solutions were then filtered through 5 μm Durapore membranes. Carbohydrate concentrations were determined by the sulfuric acid−orcinol colorimetric method.[43] Sample recoveries were calculated from the ratio of the initial mass and the mass after filtration.

AFFFF-MALLS. The AFFFF equipment, including the asymmetrical channel, Control-Box V3, Flow box P2.1, and the valve box, was obtained from Consenxus (Ober-Hilbersheim, Germany). The channel geometry was trapezoidal with a tip-to-tip length of 286 mm and breadths at the inlet and outlet of 21.2 and 4.7 mm, respectively. A 350 μm polyester spacer and a pure cellulose membrane with a cutoff point of 10 000 Da from Celgard LLB (Charlotte, NC) were used. During all AFFFF experiments, the sample was introduced into the channel using a 100 μL loop injector (Valco Instruments Co., Inc., Houston, TX). The two on-line detectors comprised a MALLS instrument (Dawn DSP-F) fitted with a K5 flow cell and an He−Ne laser ($\lambda = 632.8$ nm) (Wyatt Technology Corporation, Santa Barbara, CA) and an ERC-7515A refractometer (Erma, Tokyo, Japan). Prior to use, the carrier (Millipore water containing 0.2 g L^{-1} sodium azide) was carefully degassed and filtered through Durapore GV (0.2 μm) membranes (Millipore). The carrier was eluted initially at a flow rate of 1 mL min^{-1} for channel flow in (F_{in}). The crossflow (F_c) was then set at 1 mL min^{-1}, and the channel flow rate (F_{out}) was set at 0.2 mL min^{-1} for the sample introduction and relaxation/focusing period. The sample was injected at 0.14 mL min^{-1} for 160 s. After the injection pump was stopped, the sample was allowed to relax and focus for 60 s. For elution, F_{out} was set at 1 mL min^{-1}, and F_c was reduced from 0.4 to 0 mL min^{-1} for 400 s, after which it was maintained at 0 mL min^{-1} for 875 s. Sample recoveries were calculated from the ratio of the mass eluted from the channel (integration of the DRI signal) and the injected mass. The injected masses were determined using the sulfuric acid−orcinol colorimetric method.[43]

Data Processing. $\bar{M}_n$, $\bar{M}_w$, the polydispersity index, $\bar{M}_w/\bar{M}_n$, and $\bar{R}_G$ (nm) were established using ASTRA software from WTC (version 4.90.07 for PC).[44] After processing the light-scattering (LS) and DRI profiles using the ASTRA software, quantities c_i, M_i, and R_{Gi} (mass concentration, molar mass, and radius of gyration of the ith slice, respectively) were obtained. c_i was calculated from the DRI response. A value of 0.146 mL g^{-1} was used as the refractive index increment (dn/dc) for glucans. M_i and R_i were obtained at each slice of the elugram peak using the Berry extrapolation of the light-scattering equation (with a first-order polynomial fit) for light scattered to the zero angle

$$\sqrt{\left(\frac{Kc}{R\theta}\right)_i} = \sqrt{\frac{1}{M_i}\left(1 + \frac{16\pi^2}{3\lambda^2} R_{Gi}{}^2 \sin^2(\theta/2)\right)} \qquad (3)$$

where K is the optical constant, R_θ is the excess Rayleigh ratio of the solute, λ is the wavelength of the incident laser beam, and θ is the angle of observation. The Berry extrapolation method was used rather than classic Zimm extrapolation because it enables a more accurate extrapolation in the event of a very large polymer size.[26] Only the seven lower angles were used (from 29° to 90°) for extrapolation. $\bar{M}_n$, $\bar{M}_w$, the $\bar{M}_w/\bar{M}_n$ ratio, and $\bar{R}_G$ were calculated using the summations taken over one peak

$$\bar{M}_n = \frac{\sum_i c_i}{\sum_i c_i/M_i} \qquad (4)$$

$$\bar{M}_w = \frac{\sum_i c_i M_i}{\sum_i c_i} \qquad (5)$$

The root-mean-square z-average radius of gyration $\bar{R}_G$ was

$$\bar{R}^2_G = \frac{\sum_i c_i M_i R_{Gi}{}^2}{\sum_i c_i M_i} \qquad (6)$$

Table 1. Solubilization and Elution Recoveries, Weight Average Molar Masses ($\bar{M}_w$), *z*-Average Radii of Gyration ($\bar{R}_G$), and Polydispersity Indices ($\bar{M}_w/\bar{M}_n$) Determined by AFFFF-MALLS[a]

	solubilization recovery (%)	elution recovery (%)	$\bar{M}_w \times 10^{-8}$ (g mol^{-1})	$\bar{R}_G$ (nm)	$\bar{M}_w/\bar{M}_n$
waxy barley starch	100.0	92.7	1.88 ± 0.06	182.5 ± 1.8	1.22 ± 0.06
waxy rice starch	96.7	93.9	2.30 ± 0.17	212.2 ± 3.8	1.42 ± 0.13
waxy wheat starch	99.2	100.0	2.27 ± 0.09	198.3 ± 2.3	1.13 ± 0.06
waxy maize starch	97.7	94.8	3.18 ± 0.21	228.9 ± 3.3	1.09 ± 0.09
amf potato starch	100.0	100.0	1.05 ± 0.02	165.9 ± 1.0	1.16 ± 0.03
normal maize amylopectin	97.9	88.1	2.42 ± 0.10	207.0 ± 2.1	1.31 ± 0.07
smooth pea amylopectin	100.0	81.7	1.47 ± 0.04	163.2 ± 1.5	1.21 ± 0.07
cassava amylopectin	100.0	86.7	1.37 ± 0.04	170.7 ± 1.4	1.44 ± 0.05
rabbit liver glycogen	100.0	100.0	0.17 ± 0.02	29.5 ± 1.2	1.43 ± 0.03

[a] These values were taken over the whole peak.

An interdetector delay volume of 180 μL was determined by injecting monodispersed BSA. Normalization of the photodiodes was achieved using a low molar mass pullulan standard (P50) representative of any α-glucan.

Results and Discussion

The solubilization recovery rates (Table 1) of eight amylopectins and starches containing amylopectin only were between 96.7% for waxy rice and 100.0% for waxy barley starch, amf potato starch, smooth pea amylopectin, and cassava amylopectin (mean, 99%). Elution recoveries, which represented the percentage of macromolecules percolating through the AFFFF system, ranged from 81.7% for smooth pea amylopectin to 100.0% for amf potato starch and waxy wheat starch (mean, 92%). The high sample recovery values obtained here indicate that the fractionation response was quantitative for all of the samples. This solubilization mode was thus considered as enabling the representative structural characterization of starches.

Elugrams, Distributions, and Relations between Molar Masses and Radii. On the DRI and LS responses, a void peak appeared at an elution volume (V_0) of ~4.75 mL (Figure 1). The void peak probably contained a small part of the polymer sample. Because of the good recovery values achieved, it corresponded to a minor fraction of the polymer sample (less than 8% on average). Amylopectin and starch elugrams revealed one DRI peak and one LS peak corresponding to amylopectin which overlapped at an elution volume (V_i) of 15−16 mL, depending upon the injected sample (Figure 1). No additional peak corresponding to the amylose fraction was observed, except for waxy barley starch which presented in addition a little amylose peak at $V_i = 7.5$ mL. It should be noted that for this sample only the amylopectin peak was considered in the following.

The glycogen elugram revealed one DRI peak at an elution volume of 10 mL and one LS peak at an elution volume of 12 mL (Figure 2). The distribution of molar masses clearly demonstrated two slopes that could correspond to two components.

Both M_i (Figures 1 and 2) and R_{Gi} increased with the elution volume (V_i) for each amylopectin and glycogen population. This meant that separation took place in the normal AFFFF elution mode. AFFFF produced a good fractionation of amylopectins and glycogen that allowed us to obtain detailed macromolecular characteristics on the distributions. The relationship between the hydrodynamic radius (R_{Hi}) of fraction i and t_{ri} (or V_i) was obtained by combining the well-known Stokes−Einstein relation

$$D_i = kT/6\pi\eta R_{Hi} \quad (7)$$

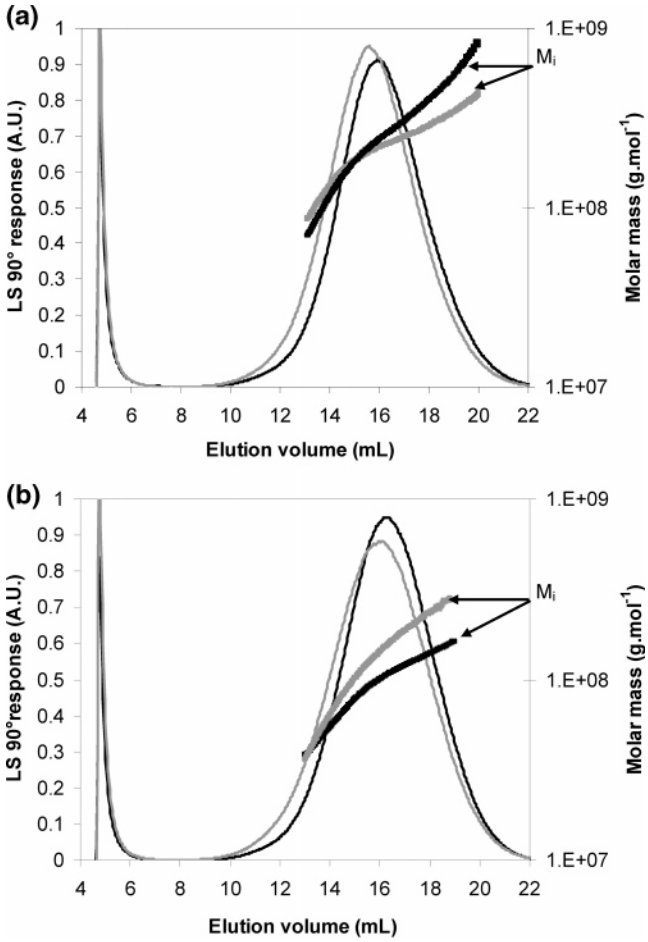

Figure 1. Elugrams (LS 90° responses) of amylopectins and their molar masses versus the elution volume (V_i): (a) waxy wheat starch (black) and waxy rice starch (gray); (b) amf potato starch (black) and cassava amylopectin (gray). The thin lines represent the LS 90° responses, and the thick lines the molar masses.

where k is the Boltzmann's constant, T the temperature, and η the viscosity of the solvent with eq 2

$$R_{Hi} = [kTV_0/t_0\pi\eta w^2 F_c(\text{start})]\{ t_{start} + (t_{end} - t_{start}) \ln[(t_{end} - t_{start})/(t_{end} - t_{ri})]\} \quad (8)$$

To use elution volumes instead of retention times, the retention times (t_{ri}) were replaced in eq 8 by elution volumes: $t_{ri} = V_i$ and $t_0 = V_0$, since $F_{out} = 1$ mL min^{-1}. For a polymer structure that remained stable throughout the distribution, the ratio between the radius of gyration and the hydrodynamic radius (ρ

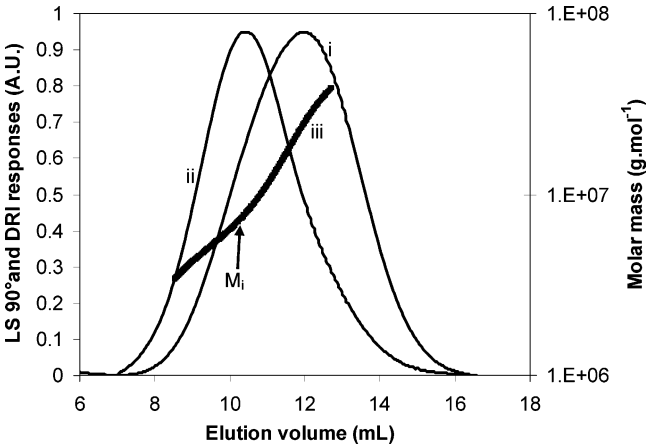

Figure 2. Elugrams (LS 90° (i) and DRI (ii) responses) of rabbit liver glycogen and its molar masses (iii) versus the elution volume (thick line).

Table 2. Structural Characteristics of the Polymers Studied: ν_G Values and Fractal Dimensions[a]

	ν_G	d_{fg}	d_{fi}
waxy barley starch	0.45	2.22	2.05
waxy rice starch	0.43	2.33	2.15
waxy wheat starch	0.44	2.27	2.17
waxy maize starch	0.37	2.70	2.52
amf potato starch	0.49	2.04	2.05
normal maize amylopectin	0.39	2.56	2.28
smooth pea amylopectin	0.43	2.33	2.12
cassava amylopectin	0.42	2.38	2.05
rabbit liver glycogen	0.68[b]/0.40[c]	1.47[b]/2.50[c]	ND[d]

[a] The experimental errors are 0.01 for ν_G values and 0.05 for fractal dimensions. [b] Value obtained from the low molar mass fraction. [c] Value obtained from the high molar mass fraction. [d] ND: not determined.

$= R_{Gi}/R_{Hi}$) could be considered as constant in a first approximation. The ρ factor depended on polymer structure. For amylopectin, the ρ values obtained were within the range of 1−1.5.[2] A power-law relationship was expected according to the empirical equation for V_i dependence of the molar mass

$$R_{Hi} = K_H M_i^{\nu H} \quad (9)$$

By plotting the gyration radius and the molar masses of the same fraction, structural data could be determined from the exponent ν_G in the equation

$$R_{Gi} = K_G M_i^{\nu G} \quad (10)$$

The values for ν_G and ν_H depended on polymer shape, temperature, and polymer−solvent interactions. $\nu_G = \nu_H = 0.33$ for a sphere, $\nu_G = \nu_H = 0.5-0.6$ for a linear random coil, and $\nu_G = \nu_H = 1$ for a rod. A very good fit of experimental data was achieved using eq 10. The ν_G values calculated from the amylopectin peak ranged from ∼0.37 to 0.49 for the amylopectins studied (Table 2). These values were in good agreement with data in the literature.[2,45] The lowest ν_G values (∼0.37) were observed for waxy maize and normal maize amylopectins. These amylopectins were therefore the most dense and probably had a high degree of branching when compared to the other amylopectins studied. The average of the ν_G values obtained for other amylopectins was 0.40, showing that these macromolecules were less dense (i.e., less branched) than those from maize. The highest ν_G value (0.49) (obtained for amf potato starch in pure water) was probably due to a polyelectrolyte effect

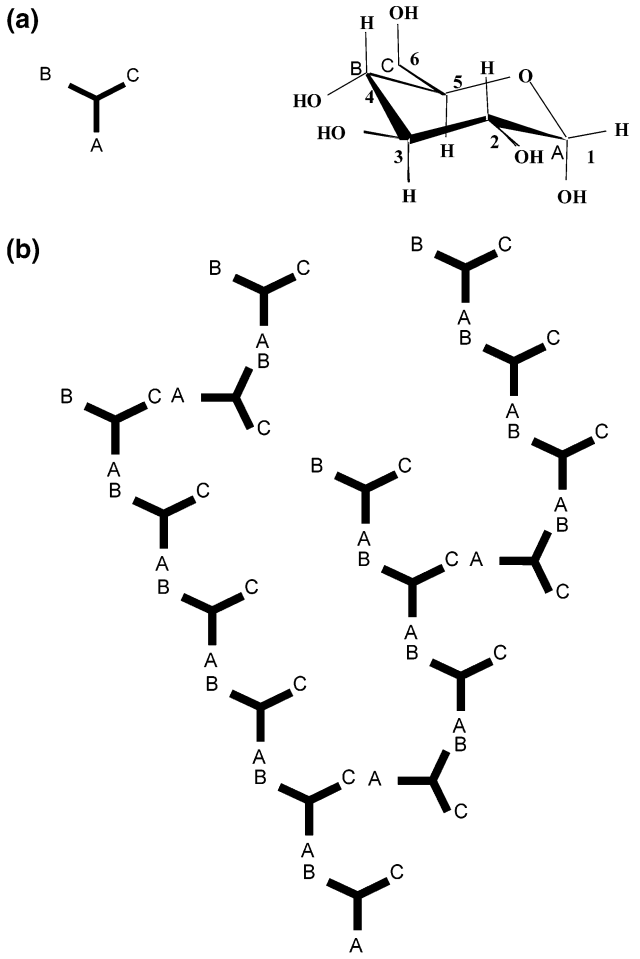

Figure 3. Glucosyl unit considered as a three-functional monomer (a) and branching in the ABC three-functional polycondensation model[40] (b).

(charge repulsion inducing an increase in the free volume of the polymer), because of the presence of phosphate groups on potato starch (0.1%).[1] With respect to rabbit liver glycogen, the plot of the radius of gyration versus the molar mass exhibited two slopes, leading to two ν_G values: 0.68 and 0.40, which corresponded to the low molar mass region and the high molar mass region, respectively (Table 2). This resulted from an overlap of two populations in the distribution. The values obtained here (Table 2) were in good agreement with data in the literature obtained for mussel glycogen (0.74 and 0.30 for the low molar mass region and high molar mass region, respectively).[41] Even though the 0.40 value was higher than the value obtained by Ioan[41] for the high molar mass fraction of glycogen (0.30), the value of 0.40 pointed to a high branching density for glycogen. This difference may have been due to the origin of the macromolecule.

Kratky Diagrams. Amylopectins and glycogen are very highly branched macromolecules, so their structure could be approached using the theory of hyperbranched macromolecules, as initiated by Flory[46] and Erlander and French.[47] Hyperbranched macromolecules are considered to arise from a polycondensation reaction of monomers containing one, so-called functional, group A and at least two other functional groups, B and C (Figure 3).

Reactions can only proceed with the focal group A and one of the two other groups, where B may have a higher reactivity than C. On average, much longer linear chain sections between branching points occur when C has a lower reactivity than B, and a strictly linear chain is obtained when the reaction of C

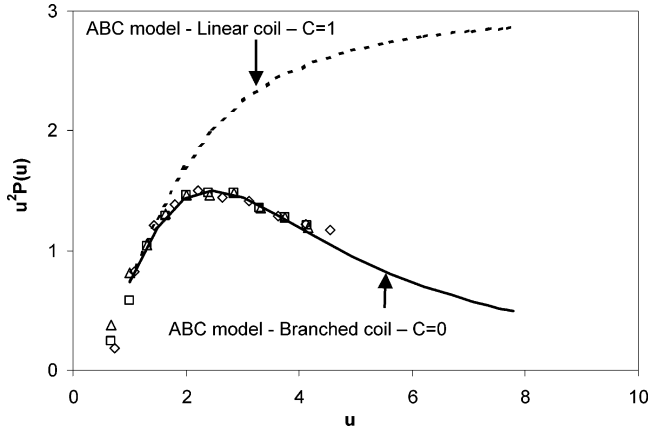

Figure 4. Kratky plots for waxy maize starch (◊), amf potato starch (□), and cassava amylopectin (△) for $R_{Gi} = 220$ nm; $u = qR_{Gi}$, q is the scattering vector magnitude. Theoretical curves are also reported according to the three-functional polycondensation ABC model for a linear coil with $C = 1$ (dotted line) and a branched coil with $C = 0$ (full line).

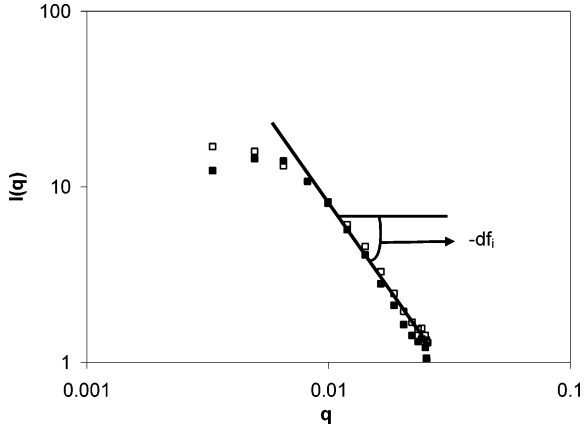

Figure 5. Plot of light scattered intensity, $I(q)$ versus the wave vector, q, for waxy barley starch (□) and normal maize amylopectin (■). Determination of d_{fi}. The line is shown as a guide.

can be fully suppressed. These structures are called hyperbranched because due to chemical constraints a very high branching density becomes possible without gelation. In this statistical model, also referred to as the ABC model proposed by Burchard,[40] the branching points are not distributed in a random way within the macromolecule. In amylopectin, the reducing end group establishes a focal end group A, which due to the specificity of biosynthesis enzymes can only react with the hydroxyl groups B and C in the C_4 and C_6 positions of the ring. A reaction with B is 25 times more frequent than one with C. If both B and C groups react, then a branching point is created. The resulting polymer presents a number average degree of polymerization ($\overline{DP}_n$) that depends on the reactivity of the focal end group. The corresponding particle scattering factor $P(u)$ was given by Burchard[48] for amylopectin

$$P(u) = (1 + Cu^2/3)/\{[1 + (1 + C)u^2/6]^2\} \qquad (11)$$

where the inverse of C denotes the number of branches of the polymer and $u = q\bar{R}_G$, with q the wave vector ($q = 4\pi n \sin(\theta/2)/\lambda$, where n is the solvent index of refraction). The scattering factor provides information on the shape of the macromolecule. The C value depends on molar mass and branching probability.[49] C has a value of 1 for a linear coil and 0 for a hyperbranched structure containing an infinite number of branching points. It is possible to approach the structure and branching of amylopectin using Kratky plots, when the scattering factor is plotted versus u.

The Kratky diagrams for amylopectins were obtained by superimposing $P(u)$ values obtained at five radii of gyration (R_{Gi}), 150, 160, 180, 200, and 220 nm, throughout the length of the elugram for the same amylopectin (Figure 4). The patterns obtained were characteristic of branched polymers, with a maximum value at $q = 2.5$. The results followed the model of hyperbranched molecules (ABC model)[48] with $C = 0$, indicating that the amylopectin fractions analyzed were highly branched so that the number of branches could not be calculated using this approach. The same patterns were obtained for all of the amylopectins studied, in each case observed at five radii of gyration. This meant that all of these amylopectins behaved like hyperbranched molecules with an infinite number of branching points throughout their distributions. It was impossible to discriminate any amylopectins using these diagrams.

Fractal Dimensions. Two fractal dimensions (d_{fg} and d_{fi}) were determined (Table 2). Considering self-similar objects (structure that independently of the length scale displays the same behavior), the fractal dimension (d_f) gives an impression of the molecular architecture.[41] Fractal dimension denotes the geometric dimension of the bodies. Because the amylopectin structure was stable throughout the distribution (linearity of R_{Gi} versus M_i), it was possible to calculate a global fractal dimension (d_{fg}).[50] Equation 10 can be rewritten as[45,50]

$$M_i = K'_G R_{Gi}^{1/\nu G} = K'_G R_{Gi}^{dfg} \qquad (12)$$

d_{fg} was obtained using the proportionality between ν_G and d_{fg} ($d_{fg} = 1/\nu_G$).[45,50]

The theory of fractals relates again the asymptotic slope of light scattered intensity $I(q)$ versus the wave vector (q) at large q values to a fractal dimension.[51] This second fractal dimension (d_{fi}) was calculated at large q values for the log $I(q)$ linear zone (Figure 5).[52] $I(q)$ describes the angular distribution of scattered light, so d_{fi} values make it possible to obtain structural features free of $\bar{M}_w$ and $\bar{R}_G$.

In fact, amylopectin could not be considered as having a simple fractal structure.[24] For intermediate $q\bar{R}_G$ values (up to 8), the observation window corresponded to several branching generations at a scale higher than the cluster. This led to different slopes for $I(q)$ versus q, and only a small q domain (lower than one decade) enabled the observation of a fractal object, in agreement with the theory of hyperbranched macromolecules.[24] So, in the present experimental $q\bar{R}_G$ range (up to 6), d_{fi} was found from the internal structure and corresponded to several branching generations at a scale higher than the cluster contrasted with d_{fg}, which was related to the global structure.[45]

The d_{fi} values were between those obtained for a statistically branched molecule swollen in a good solvent ($d_f = 2$) and those specific to a nonswollen branched coil ($d_f = 2.5$). These values were close to those obtained previously for waxy maize and potato amylopectin without fractionation of the macromolecules[2] or after HPSEC separation[5] or sedimentation FFF separation.[45] It was then possible to classify the amylopectins as a function of their swelling in the solvent. The d_{fg} values were systematically higher than the d_{fi} values, except for amf potato amylopectin. The d_{fg} values exhibited the same tendency as d_{fi} and were close to 2.5, thus highlighting highly branched molecules, except for cassava, waxy barley, and amf potato amylopectins, which revealed behavior similar to that of statistically branched molecules swollen in a good solvent. The exception was waxy maize amylopectin ($d_f > 2.5$), which had a fractal dimension close to 3, this value being characteristic of a compact sphere

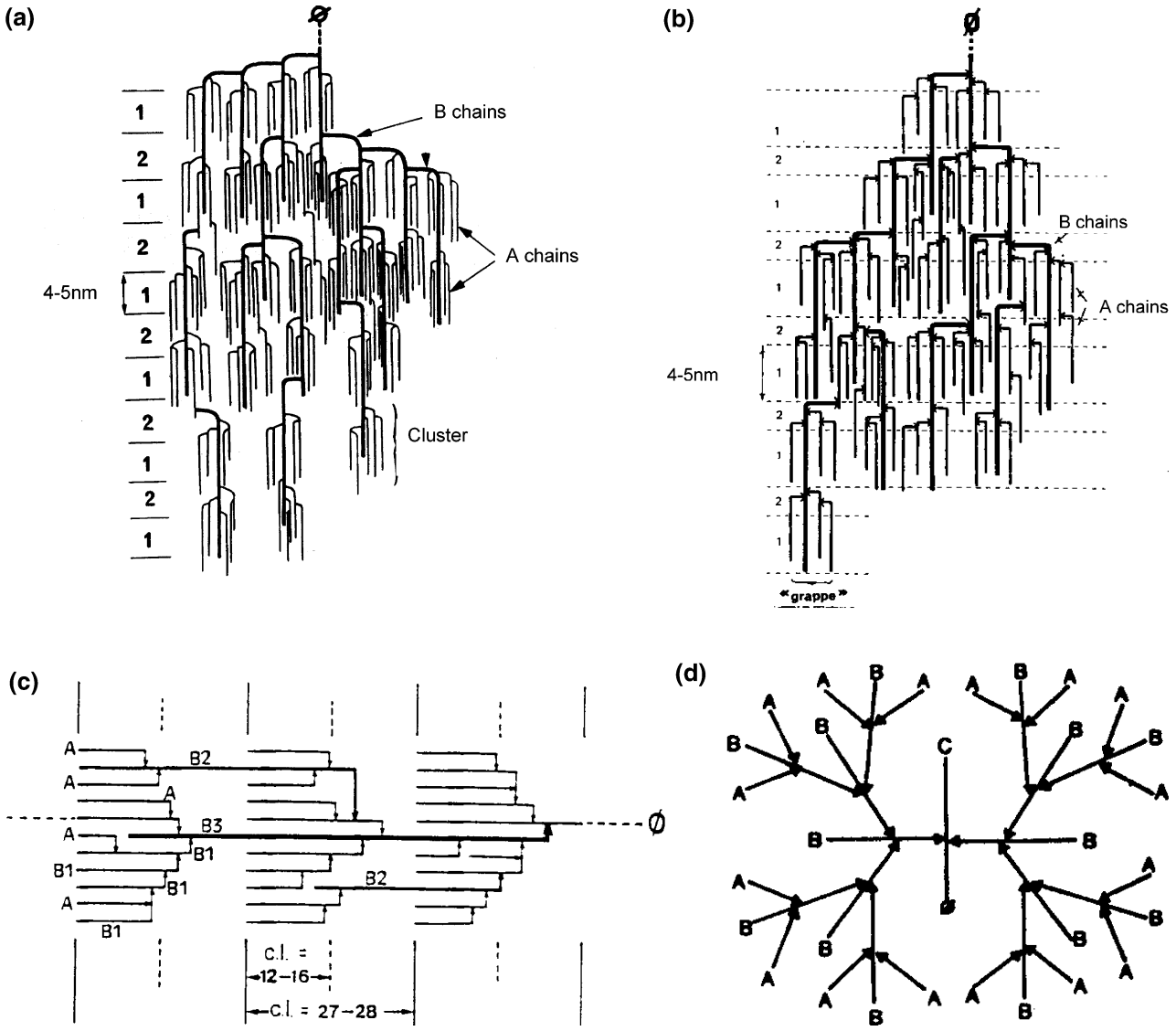

Figure 6. Amylopectin and glycogen structures. These two α-glucans are both mainly built upon α-(1,4) linkages and have a branched structure with 5−6% and 8% α-(1,6) linkages, respectively, for amylopectin[1] and glycogen.[41] (a) Amylopectin structure according to French[27] and Robin[28] for waxy maize amylopectin; (b) amylopectin structure according to French[27] and Robin[28] for potato amylopectin; (c) amylopectin structure according to Hizukuri;[36] and (d) glycogen Whelan structure.[42]

(indicating its very high branching density). The differences between d_{fg} and d_{fi} could be explained by heterogeneity in the amylopectin structure. According to these fractal dimensions, the internal structure appeared to be less branched than that shown by the global structure. These findings were in agreement with the cluster model for amylopectin architecture,[28,36,37,52] which contrasts with the compact and homogeneous Whelan structure proposed previously for glycogen[42] (Figure 6 d). The exception was again amf potato amylopectin, for the reasons mentioned above. Thus, the greater the difference between d_{fg} and d_{fi}, the more heterogeneous the amylopectin structure. Normal maize and cassava amylopectins revealed the most heterogeneous structures, followed by waxy barley, rice, maize starches, smooth pea amylopectin, and finally waxy wheat starch, which appeared to have the least heterogeneous structure. These differences could be related to the lengths of the internal linear chains of amylopectin.

Average Molar Masses, Radii, and Branching Parameters. Amylopectin $\bar{M}_w$ and $\bar{R}_G$ ranged from 1.05 to 3.21 × 10^8 g mol^{-1} and from 163 to 229 nm, respectively (Table 1). These values were close to those previously obtained by HPSEC and were in good agreement with data in the literature.[2,4,15,45] Maize amylopectins exhibited the highest $\bar{M}_w$ and $\bar{R}_G$ values, followed by waxy wheat amylopectin, waxy rice amylopectin, cassava and smooth pea amylopectins, and finally amf potato amylopectin, which had the lowest $\bar{M}_w$ and $\bar{R}_G$ values (Table 1). $\bar{M}_w$ and $\bar{R}_G$ were 1.39 × 10^7 g mol^{-1} and 28.7 nm, respectively, for rabbit liver glycogen.

The average shrinking factor g_M (or branching parameter) was defined[23] as the ratio between the mean-square radius of gyration of branched and linear polymers with the same molar mass

$$g_M = \bar{R}^2_{Gw(br)}/\bar{R}^2_{Gw(lin)} \quad (13)$$

where $\bar{R}_{Gw}$ are the weight average radii of gyration, the subscripts br and lin denoting branched polymer and corresponding linear one, respectively. g_M was calculated using the ratio of $\bar{R}^2_{Gw(br)}/\bar{R}^2_{Gw(lin)}$ determined by AFFFF-MALLS for macromolecules with a molar mass $\bar{M}_w$. $\bar{R}^2_{Gw(lin)}$ was determined for each sample using the relationship established for synthetic

Table 3. Branching Parameters Determined by the Simple ABC Model as Proposed by Burchard[48,49] Using Eq 15[a]

	g_M	$\bar{B}$	$\bar{B}/\overline{DP}_w$	$\overline{DP}_w/\bar{B}$	BD (%)
waxy barley starch	0.031	7636.3	0.007	151.6	0.7
waxy rice starch	0.030	8266.7	0.006	171.3	0.6
waxy wheat starch	0.031	8094.8	0.006	172.7	0.6
waxy maize starch	0.027	10096.0	0.005	194.0	0.5
amf potato starch	0.055	2392.4	0.004	270.3	0.4
normal maize amylopectin	0.030	8586.8	0.006	173.6	0.6
smooth pea amylopectin	0.035	6221.8	0.007	145.5	0.7
cassava amylopectin	0.041	4388.1	0.005	188.1	0.5
rabbit liver glycogen	0.012	52522.0	0.495	2.0	49.5

[a] Average shrinking factor (g_M), average number of branching points ($\bar{B}$), branching probability ($\bar{B}/\overline{DP}_w$), average number of glucosyl units in a linear chain per branching point ($\overline{DP}_w/\bar{B}$) and branching degree (BD).

amyloses in aqueous media (Rolland-Sabaté et al., results to be published)

$$\bar{R}_{Gw(lin)} = 5.96 \times 10^{-3}\, \bar{M}_w^{\,0.63} \qquad (14)$$

The average shrinking factors g_M rose from 0.027 for waxy maize amylopectin to 0.055 for amf potato amylopectin (Table 3). It was shown previously[22] that in amylopectin and glycogen the g_M value fell when the average branching degree increased and that the average branching degree increased in line with the molar masses. It should then have been possible to rank the amylopectins in terms of their branching degrees as a function of their average g_M values. The amf potato amylopectin appeared to be the least branched amylopectin and with the highest g_M value, in contrast to waxy maize amylopectin, which was the most branched amylopectin. Glycogen exhibited the lowest average g_M value, in agreement with its branching degree (8.0%)[41] and in contrast with that of waxy maize amylopectin (4.8%).[39] The g_M values obtained were consistent with the other structural characteristics determined (ν_G values and fractal dimensions). In the case of amylopectin, the ABC three-functional polycondensation model (ABC model) gave, for g_M[48,49]

$$g_M = \bar{R}^2_{Gw(br)}/\bar{R}^2_{Gw(lin)} = 4\{[(1+2\bar{B})^{1/2}]/[1+(1+2\bar{B})^{1/2}]^2\} \qquad (15)$$

where $\bar{B}$ is the average number of branching points. From eq 15, it was then possible to determine the number of branching points per macromolecule. The average number of glucosyl units per branching point (for two arms) was represented by the ratio $\overline{DP}_w/\bar{B}$. The average number of branching points for amylopectins, $\bar{B}$, decreased from 1.01×10^4 for waxy maize to 0.24×10^4 for amf potato amylopectin (Table 3). $\overline{DP}_w/\bar{B}$, corresponding to an average chain length, increased from 145.5 for smooth pea amylopectin up to 270.3 for amf potato amylopectin. These values were lower than those obtained previously by Aberle.[26] However, they were higher than the values of the average chain length ($\overline{CL}$), 18−34, determined previously[53−56] after debranching of the samples. The branching degree as determined by NMR is the ratio of the number of α-(1,6) linkages to the total number of links in the molecule,[39] so the value of the branching degree determined by NMR could be compared to the branching degree determined using the ABC model. The average branching degrees obtained for the amylopectins studied, when fitting the data with the ABC model, were very low (lower than 1%) when compared with the branching degree determined previously by NMR: 4.8% and 4.1% for waxy maize and potato amylopectins, respectively.[39] However, amf potato amylopectin appeared to be the least branched, with a longer chain length, in contrast to smooth pea and waxy barley amylopectins, which exhibited the highest degree of branching. Waxy maize amylopectin appeared to be more branched than amf potato amylopectin, so the amylopectin branching degrees determined by this method followed the same order as the branching degrees obtained by NMR.[39] And even if the shrinking factors determined were consistent with other structural characteristics, the branching degrees obtained with the ABC model and applied to AFFFF-fractionated amylopectins were not consistent with the branching degrees obtained by NMR[39] or after sample deramification.[53−56] The ABC model thus underestimated the number of branching points of amylopectins, as had already been suggested.[24,25] The explanation given for this was the heterogeneity of amylopectin branching, the excluded volume effect (which was not incorporated into the theory), and a neglect of chain stiffness.[24,25,57] The branching degree obtained for glycogen was extremely high when compared with the value of 8.0% previously determined chemically for glycogen.[41] This overestimation was in agreement with results obtained previously for nonfractionated glycogens using the ABC model.[41] One possible explanation for this could again be the heterogeneity of branching density linked to glycogen biosynthesis, which is probably much more complex than the idealized model used, which was based on a statistical process.[41]

If the Robin[28] model for amylopectin structure is considered (Figures 6a and 6b), then each B chain carries two clusters with 3 and 4.5 chains per cluster for potato and waxy maize amylopectins, respectively (corresponding to 7 and 10 chains per B chain group, including the B chain). In view of the fact that previous calculations using the ABC model could only detect the branching points between long B chains, and then multiplying $\bar{B}$ by 7 and 10, respectively, it would thus be possible to obtain the "total" number of branching points in the macromolecule. Applying this model (Table 4), the average numbers of glucosyl units in a linear chain per branching point ($\overline{DP}_w/\bar{B}_{mR}$)were 38.6 and 19.4 for amf potato and waxy maize amylopectins, respectively. In Table 4, values are calculated using a mean value for the number of chains per B group (8.50). These modified values for chain length ($\overline{DP}_w/\bar{B}_{mR}$) and branching degree ($BD_{mR}$) were entirely consistent with the values obtained previously by NMR[39] or after debranching.[53−56]

When considering the Hizukuri[36] model for amylopectin structure (Figure 6c), each B3 chain carries 14 A and B1 chains and two B2 chains each carry 4 A and B1 chains; thus each long B chain (B2 + B3) carries 8.33 chains on average. Under this model, the average numbers of glucosyl units in a linear chain per branching point ($\overline{DP}_w/\bar{B}_{mH}$) were between 32.4 and 17.5 for potato and smooth pea amylopectins, respectively (Table 4). These modified chain length ($\overline{DP}_w/\bar{B}_{mH}$) and branching degree values (BD_{mH}) were in agreement with the results obtained previously by NMR[39] or after debranching[53−56] and were very close to those obtained with the Robin model (Table 4). So, in the figures that follow, the "modified" ABC model corresponds to a model where $\bar{B}$ values were calculated using the Hizukuri structure, multiplying $\bar{B}$ values obtained with eq 15 by a factor of 8.33 to obtain the "total" number of branching points.

The branching degrees obtained placed most amylopectins in the same order as that reported in the literature.[39,53−56] Surprisingly, waxy maize amylopectin, which had the highest number of branching points (Table 3) and exhibited the highest density in terms of fractal dimensions (Table 2), did not

Table 4. Modified Values for the Average Number of Glucosyl Units in a Linear Chain per Branching Point ($\overline{DP}_w/\bar{B}_{mR}$ and $\overline{DP}_w/\bar{B}_{mH}$), the Average Number of Branching Points ($\bar{B}_{mR}$ and $\bar{B}_{mH}$), and the Branching Degree (BD_{mR} and BD_{mH}) Using Theoretical Amylopectin Structures as Proposed by Robin[28] and Hizukuri[36a]

	Robin model[b]			Hizukuri model		
	$\overline{DP}_w/\bar{B}_{mR}$	$\bar{B}_{mR}$	BD_{mR} (%)	$\overline{DP}_w/\bar{B}_{mH}$	$\bar{B}_{mH}$	BD_{mH} (%)
waxy barley starch	17.8	6.5×10^4	5.6	18.2	6.4×10^4	5.5
waxy rice starch	20.2	7.0×10^4	5.0	20.6	6.9×10^4	4.9
waxy wheat starch	20.3	6.9×10^4	4.9	20.7	6.8×10^4	4.8
waxy maize starch[b]	22.8	8.6×10^4	4.4	23.3	8.4×10^4	4.3
	(19.4)	(10.0×10^4)	(5.2)			
amf potato starch[b]	31.8	2.0×10^4	3.1	32.4	2.0×10^4	3.1
	(38.6)	($1.7 \times 10^{4)}$	(2.6)			
normal maize amylopectin	20.4	7.3×10^4	4.9	20.8	7.2×10^4	4.8
smooth pea amylopectin	17.1	5.3×10^4	5.8	17.5	5.2×10^4	5.7
cassava amylopectin	22.1	3.7×10^4	4.5	22.6	3.7×10^4	4.4

[a] The subscripts mR and mH denote the values obtained after calculations using theoretical amylopectin structures as proposed by Robin and Hizukuri respectively. [b] Under the Robin model, a mean value was used for comparisons between samples, the values in parentheses representing the values calculated according to the Robin structures proposed for waxy maize (see Figure 6 a) and potato (see Figure 6 b) amylopectins, respectively.

demonstrate the highest branching degree. Another interesting inconsistency was that smooth pea amylopectin presented the highest branching degree (Table 4), even though its shrinking factor and fractal dimensions (Table 2) showed that this molecule was not the most dense.

Applying the ABC model to amylopectin thus did not allow determination of the total branching degree of this molecule. This method only highlighted the branching points corresponding to longer linear B chains, i.e., the number of B chain bearing cluster anchorage points. The branching points belonging to clusters were not observed. Thus, working with native amylopectins, it was impossible to access the branching density of clusters using this technique. The branching values determined using the ABC model corresponded to internal branching characteristics and also included structural information on clusters, but a separate study was impossible. For most of the amylopectins studied, $\bar{B}$ values were in the same order as d_{fi} values; the higher the $\bar{B}$, the higher the d_{fi} (Tables 2 and 3). This confirmed that $\bar{B}$ contained information about the internal structure of amylopectin, such as long-chain branching. It was thus possible to rank the amylopectins as a function of their internal branching density using $\bar{B}$ values; the higher the $\bar{B}$ values, the higher the number of anchorage points of B chains carrying the clusters, or long-chain branching density. However, by applying the ABC model while taking account of known amylopectin structures, it was possible to determine the average branching degree values for amylopectins, in line with data in the literature.[39,53−56]

The plot of g_M versus the average number of branching points ($\bar{B}$) (Figure 7) shows the difference between the ABC model and "modified" ABC model. The $\bar{B}$ values calculated from corresponding data in the literature[39,53−56] are also reported. The latter fitted well with the "modified" ABC model for amylopectins, but the fit with ABC models was particularly poor for glycogen. Thus, for amylopectins, the relationship between g_M and the number of branches was approached using the "modified" ABC model, but no clear link was found between g_M and the branching degree (results not shown). The model used was however simple for amylopectins. Amylopectin branching structures were heterogeneous and differed as a function of botanical origin, as shown by the two models proposed for waxy maize and potato amylopectin by Robin[28] (Figures 6a and 6b). However, in the model used, the same "mean" amylopectin branching structure was considered for all of the samples. A more complicated model including these differences in the calculations would improve the determination of the branching degree.

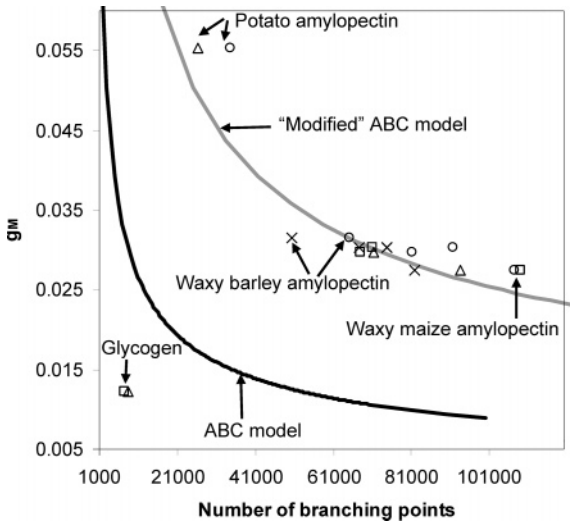

Figure 7. Average shrinking factor (g_M) versus the average number of branching points ($\bar{B}$) according to the ABC model (black line) and the "modified" ABC model (gray line). Corresponding data from the literature are also reported. Chemical data[41] for glycogen, NMR[39] data for waxy maize, normal maize, and potato amylopectins (△); debranching data from Caldwell and Matheson[55] for waxy maize, normal maize, waxy rice, waxy barley, and waxy potato amylopectins (○); debranching data from Shi and Seib[54] for waxy maize, waxy rice, and waxy barley amylopectins (×); debranching data from Yun and Matheson[56] for glycogen, waxy maize, normal maize ,and waxy rice amylopectins (□). The values of the average number of branching points calculated from the literature were obtained by combining the $\overline{DP}_w$ value determined here for each macromolecule and corresponding data from the literature.[39,41,54,55,56] In the "modified" ABC model, $\bar{B}$ values were calculated using the Hizukuri structure,[36] multiplying $\bar{B}$ values obtained with eq 15 by a factor of 8.33 to obtain the "total" number of branching points.

Branching Parameter Distributions. Zimm and Stockmayer developed an equation using a random three-functional polycondensation model, based on a linear growth of chain branches. The branches become forked at the same average length with a given probability, and this occurs for each new branch generation. In the case of narrow polymer fractions, the shrinking factor of the ith slice (g_i) is thus given by[23]

$$g_i = R^2_{Gi(br)}/R^2_{Gi(lin)} = [(1 + n_i/7)^{1/2} + 4n_i/9\pi]^{-1/2} \quad (16)$$

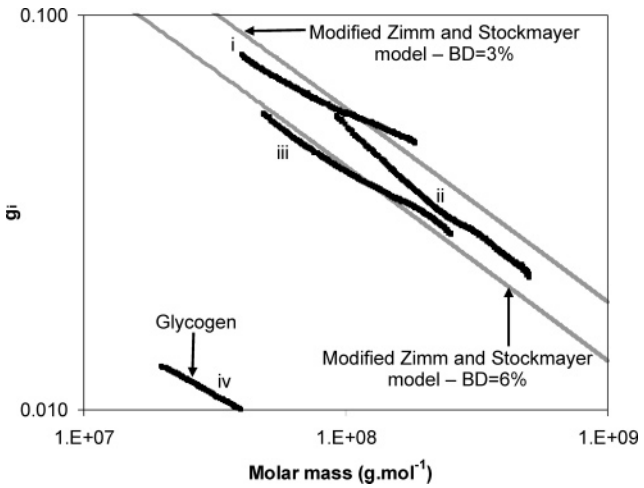

Figure 8. Shrinking factor (g_i) versus molar mass (M_i) along the distributions for amf potato (i), smooth pea (ii), and waxy maize (iii) amylopectins and glycogen (iv). The gray lines represent the theoretical response of the "modified" Zimm and Stockmayer model for two branching degrees (BDs) constant along the distribution 3% (up) and 6% (down). The "modified" Zimm and Stockmayer model corresponds to a model where n_i values were calculated using the Hizukuri structure,[36] multiplying n_i values obtained with eq 16 by a factor of 8.33 to obtain the "total" number of branching points.

where n_i is the number of branching points of the ith slice. From eq 16, it is then possible to determine the number of branching points per macromolecule for each slice of the elugrams.Considering a constant branching degree along the whole distribution, one could postulate

$$g_i = [(1 + M_i/7M_0)^{1/2} + 4\,M_i/9\pi M_0]^{-1/2} \qquad (17)$$

with $M_i = M_0 n_i$ and M_0 the molar mass per branching unit. From eq 17, one could determine the molar mass of one branching unit (M_0) and then the average number of glucosyl units per branching point (DP_0), which corresponds to the ratio $\overline{DP_w}/\bar{B}$. It previously has been shown that the shrinking factor has a dependence on the number of branching points, which is very similar with the ABC three-functional polycondensation model and the Zimm and Stockmayer model,[26] the curves overlapping for a number of branching points higher than 10^2. For this reason, the Zimm and Stockmayer equation was used for slice analyses.

The plot of experimental g_i versus molar mass (M_i) along the distributions showed that g_i decreased when the molar mass increased (Figure 8). These results were consistent with those previously obtained on nonfractionated hydrolyzed amylopectins.[25] The Zimm and Stockmayer equation approached a power-law dependence for g_i versus molar mass (M_i) with an exponent of -0.5, and the position of the "modified" Zimm and Stockmayer model theoretical curve depended on the branching degree (Figure 8). The "modified" Zimm and Stockmayer model corresponded to a model where n_i values were calculated using the Hizukuri structure,[36] multiplying n_i values obtained with eq 16 by a factor of 8.33 to obtain the "total" number of branching points. Amylopectin g_i distributions were between the "modified" Zimm and Stockmayer model theoretical curves corresponding to branching degrees of 3% and 6%, which was in line with the results obtained on average values using the "modified" ABC model. Using all of the amylopectin data, a power-law dependence for g_i versus M_i with an exponent of -0.46 rather than -0.5 was found with an r^2 of 0.83. In fact, the decrease of g_i with M_i differed for each amylopectin. A better fit was obtained if the exponent -0.5 was changed to a free parameter. This exponent was obtained from the slope of the log−log plot of g_i versus molar mass (Figure 8 and Table 5). The exponents obtained ranged from -0.3 for barley and potato amylopectins to -0.5 for waxy and normal maize amylopectins (Table 5). According to these results, maize amylopectin data fitted well to the "modified" Zimm and Stockmayer model, in contrast with other amylopectins and glycogen. The change in this exponent could be due to differences in the amylopectin branching structures as a function of botanical origin. It was noticeable that for amylopectins, these exponents were ranked the same way as d_{fg}; i.e., the lower the exponent, the higher the d_{fg} (Tables 2 and 5). This exponent may therefore be linked to the global amylopectin structure. The g_i plot for glycogen was clearly below the amylopectin g_i plots, thus emphasizing its very high branching density and/or very different branching pattern.

Table 5. Exponent of the Power-Law Relation between the Shrinking Factor (g_i) and the Molar Mass (M_i) Obtained from the Slope of the Log−Log Plot of g_i versus M_i for Amylopectins and Glycogen

	exponent of the power-law relation between g_i and M_i
waxy barley starch	−0.31
waxy rice starch	−0.38
waxy wheat starch	−0.34
waxy maize starch	−0.51
amf potato starch	−0.32
normal maize amylopectin	−0.48
smooth pea amylopectin	−0.39
cassava amylopectin	−0.45
rabbit liver glycogen	−0.37

Table 6. Molar Mass of a Branching Unit (M_0), Number of Glucosyl Units in a Linear Chain per Branching Unit (DP_0), and Branching Degree BD (BD_{ZSE}) Determined for the Amylopectins Studied Using the Zimm and Stockmayer Equation, Replacing the Exponent −0.5 by the Corresponding Exponent Determined for Each Amylopectin (Table 5)

	M_0	DP_0	BD_{zse} (%)
waxy barley starch	358	2.2	45.3
waxy rice starch	3280	20.2	4.9
waxy wheat starch	1156	7.1	14.0
waxy maize starch	36209	223.5	0.5
amf potato starch	1037	6.4	15.6
normal maize amylopectin	24782	153.0	0.7
smooth pea amylopectin	3957	24.4	4.1
cassava amylopectin	14988	92.5	1.1

Branching degrees (BD_{ZSE}) were calculated fitting eq 17 with the corresponding exponents determined for each amylopectin and glycogen (Tables 5 and 6). BD_{ZSE} values ranged from 0.5% to 45.3% in waxy maize and barley amylopectins, respectively. Branching degrees were underestimated for waxy maize, normal maize, and cassava (as in the simple ABC model) and overestimated for potato, wheat, and barley amylopectins when compared with data in the literature.[39,53−56] Rice and smooth pea amylopectins presented values closer to those in the literature. The BD_{ZSE} value obtained for glycogen was overestimated (value higher than 100%). Thus changing the various exponents for the power-law linking g_i and the number of branching points was not sufficient to take account of branching heterogeneity in the calculations.

Optimization of the Procedure. Different analytical conditions were tested before choosing the method described in the

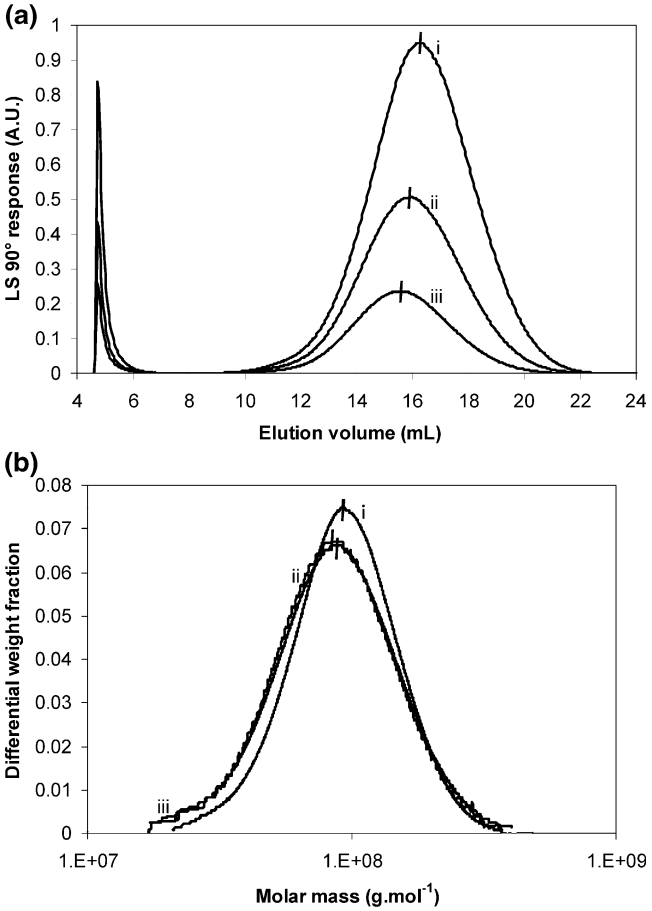

Figure 9. Overloading effect. (a) Normalized light-scattering response of amf potato starch at three different injected concentrations: 0.50 g L^{-1} (50 μg) (i), 0.25 g L^{-1} (25 μg) (ii), 0.10 g L^{-1} (10 μg) (iii). (b) Differential molar mass distribution of amf potato starch at the three different injected concentrations: 0.50 g L^{-1} (50 μg) (i), 0.25 g L^{-1} (25 μg) (ii), 0.10 g L^{-1} (10 μg) (iii). The corresponding injected masses are in parentheses.

Experimental Section. Various elution conditions were tested with F_{out} set at 1 mL min^{-1}. A constant F_c was shown to be unsuitable for amylopectin fractionation: The peaks were very broad even at an F_c of 0.2 mL min^{-1}. A linear F_c gradient was more appropriate in that case. The F_c(start) and gradient slope were adjusted from 1 to 0.2 mL min^{-1} and from 50 to 200 s per 0.1 mL min^{-1}, respectively, to determine the optimum separation conditions, as described in the Experimental Section. And to evaluate the overloading effect, amylopectins were injected at three different concentrations (0.50, 0.25, and 0.10 g L^{-1}) (Figure 9). The classic AFFFF retention model could not cope with high polymer concentrations, as interactions between neighboring particles could modify their spatial distribution. This overloading effect has been described for certain polymers (polystyrenes, glutenin, cellulose, and cationic potato amylopectin) and particles (hard spheres): It causes distorted elugrams and earlier or later retention times depending on the analyte and elution conditions.[6,9,19,20,58−60] Overloading may result in an absence of fractionation of the polymer and affect the determination of molar mass and hence structural data.[9] Retention times and elution recoveries were the same at the three concentrations. Molar masses and polydispersities were very similar at the three concentrations (Figure 9). These observations mean that the overloading effect was limited. In fact, the limiting factor was the refractometric response. With low injected masses, refractometric responses were noisy because they were very close to the refractometer detection limit

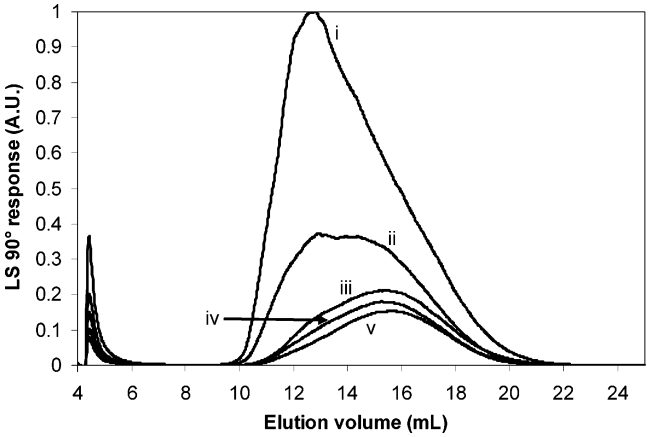

Figure 10. Light-scattering response for waxy maize starch injected at five different concentrations: 0.50 g L^{-1} (50 μg) (i), 0.25 g L^{-1} (25 μg) (ii), 0.16 g L^{-1} (16 μg) (iii), 0.10 g L^{-1} (10 μg) (iv), and 0.08 g L^{-1} (8.0 μg) (v). Corresponding injected masses are in parentheses.

and caused noisy signals affecting the radii and masses. The final concentration chosen was 0.50 g L^{-1}, corresponding to an injected mass of 50 μg.

Additional Remarks. It should be noted that after replacing the membrane with a new one differences were observed between the elugrams. The overloading effect occurred earlier and caused peak distortion as from the injection of 16 μg (Figure 10). Recovery rates were lower (~80%), but the average molar masses obtained were the same when 16 μg was injected. The second membrane was not obtained from the same supplier but from Millipore. The differences observed may have been due to the membrane supplier. In fact, differences in the membrane surface may have explained this behavior: Interactions between the sample and membrane were more marked in the case of the Millipore membrane (lower recovery), so sample retention behavior differed.

Conclusions

AFFFF-MALLS enabled the structural characterization of amylopectins, including their branching features, and highlighted the differences between them as a function of botanical origin. These findings agreed well with other data in the literature. One of the advantages of this method was that it was less time-consuming than the other methods generally used to study the structures of amylopectins. Maize amylopectins were the largest, most dense, and most branched. By contrast, amf potato starch was the smallest, least dense, and least branched amylopectin. The other amylopectins studied presented intermediate values for mass, size, and density. It was more difficult to determine differences between them because these values were less contrasted. Waxy barley, waxy rice starches, and smooth pea amylopectin were highly branched. Comparisons of fractal dimensions d_{fi} and global fractal dimensions (d_{fg}) made it possible to highlight differences between internal and global amylopectin structures as a function of botanical origin. The structure of waxy wheat starch appeared to be more homogeneous than those of the other amylopectins studied, while normal maize and cassava amylopectins appeared to be the most heterogeneous.

Using the ABC model, which took into account known amylopectin structures (the "modified" ABC model), it was possible to evaluate the amylopectin branching degree with results that agreed well with those in the literature.[39,53−56] The

inconsistencies highlighted for waxy maize and smooth pea amylopectins could be explained by the model used, which considered the same branching structure for all amylopectins. Thus this only provided an evaluation of the total branching degree of amylopectins. It was possible to rank the amylopectins as a function of the number of the anchorage points of B chains carrying the clusters (or long-chain branching density) using $\bar{B}$ values: amf potato starch < cassava amylopectin < smooth pea amylopectin < waxy barley starch, waxy wheat starch, waxy rice starch, normal maize amylopectin < waxy maize starch. Nevertheless, on the basis of native amylopectins, the ABC model did not generate detailed information on cluster branching patterns because it did not take into account the amylopectin branching pattern. The relationship between the shrinking factor and molar mass differed in all of the amylopectins studied, probably because their structures differed as a function of their botanical origin. However, taking into account the exponents linking the shrinking factor and the molar mass did not improve determinations of the branching degree using the ABC and Zimm and Stockmayer models.

Acknowledgment. We are very grateful to Professor Burchard for his valuable advice concerning structural characteristics. We thank the Conseil Régional des Pays de la Loire for its financial support under the VANAM II program.

List of Symbols

$\bar{B}$, average number of branching points in the ABC three-functional polycondensation model (eq 15)

$\bar{B}_{mH}$, average number of branching points obtained using theoretical amylopectin structures as proposed by Hizukuri

$\bar{B}_{mR}$, average number of branching points obtained using theoretical amylopectin structures as proposed by Robin

BD, branching degree

BD_{mH}, branching degree obtained using theoretical amylopectin structures as proposed by Hizukuri

BD_{mR}, branching degree obtained using theoretical amylopectin structures as proposed by Robin

BD_{ZSE}, branching degree obtained using the Zimm and Stockmayer equation

$\bar{B}/\overline{DP}_w$, branching probability

C, the inverse of C denotes the number of branches of the polymer (eq 11)

c_i, mass concentration of the ith slice.

$\overline{CL}$, average chain length.

d_{fg}, d_{fi}, fractal dimensions.

D_i, translational coefficient of diffusion of the ith slice

dn/dc, refractive index increment

$\overline{DP}_0$, average number of glucosyl units per branching point

$\overline{DP}_n$, number average degree of polymerization

$\overline{DP}_w$, weight average degree of polymerization

$\overline{DP}_w/\bar{B}$, average number of glucosyl units in a linear chain per branching point

$\overline{DP}_w/\bar{B}_{mH}$, average number of glucosyl units in a linear chain per branching point obtained using theoretical amylopectin structures as proposed by Hizukuri

$\overline{DP}_w/\bar{B}_{mR}$, average number of glucosyl units in a linear chain per branching point obtained using theoretical amylopectin structures as proposed by Robin

F_c, crossflow rate

F_c(start), crossflow rate at the beginning of the gradient

F_{in}, channel flow in

F_{out}, channel flow rate

g_i, shrinking factor or branching parameter of the ith slice

g_M, average shrinking factor or average branching parameter

g_v, ratio between the molar mass of the linear and branched polymer at the same elution volume

η, viscosity of the solvent

$I(q)$, light scattered intensity

k, Boltzmann's constant

K, optical constant

K_G, K_H, K'_G, constants

λ, wavelength of the incident laser beam

M_i, molar mass of the ith slice

M_0, molar mass per branching unit

$\bar{M}_n$, number average molar mass

$\bar{M}_w$, weight average molar mass

$\bar{M}_w/\bar{M}_n$, polydispersity index

ν_G, ν_H, hydrodynamic coefficients

N, solvent index of refraction

n_i, number of branching points of the ith slice in the Zimm and Stockmayer equation (eq 16)

$P(N)$, number of chains with a degree of polymerization N

$P(u)$, particle scattering factor

q, wave vector, $q = 4\pi n \sin(\theta/2)/\lambda$.

ρ, structure factor, $\rho = R_{Gi}/R_{Hi.}$

R, retention time

$\bar{R}_G$, z-average radius of gyration

R_{Gi}, radius of gyration of the ith slice

$\bar{R}_{Gw(br)}$, weight average radius of gyration of the branched polymer

$R_{Gi(br)}$, radius of gyration of the ith slice for the branched polymer

$\bar{R}_{Gw(lin)}$, weight average radius of gyration for the corresponding linear polymer

$R_{Gi(lin)}$, radius of gyration of the ith slice for the corresponding linear polymer

$\bar{R}_H$, average hydrodynamic radius

R_θ, excess Rayleigh ratio of the solute

T, temperature

t_{end}, time corresponding to the end of the gradient

θ, angle of observation

t_0, void time

t_{ri}, retention time of the ith slice

t_{start}, time corresponding to the start of the gradient

$u = q\bar{R}_{G.}$

V_0, void volume

V_i, elution volume of the ith slice

w, channel thickness

References and Notes

(1) Buléon, A.; Colonna, P.; Planchot, V. and Ball, S. *Int. J. Biol. Macromol.* **1998**, *23*, 85−112.
(2) Roger, P.; Bello-Pérez, L. A.; Colonna, P. *Polymer* **1999**, *40*, 6897−6909.
(3) Striegel, A. M.; Timpa, J. D. *Carbohydr. Res.* **1995**, *267*, 271−290.
(4) Bello-Pérez, L. A.; Roger, P.; Baud, B.; Colonna, P. *J. Cereal Sci.* **1998**, *27*, 267−278.
(5) Baud, B. Ph.D. Thesis, University of Nantes, Nantes, France, 1999.
(6) Martin, M. *Adv. Chromatogr.* **1998**, *39*, 1−138.
(7) Litzén A. *Anal. Chem.* **1993**, *65*, 461−470.
(8) Wahlund, K. G.; Giddings, J. C. *Anal. Chem.* **1987**, *59*, 1332−1339.
(9) Wittgren, B.; Wahlund, K. G. *J. Chromatogr., A* **1997**, *791*, 135−149.
(10) Wittgren, B.; Wahlund, K. G.; Dérand, H.; Wesslén, B. *Macromolecules* **1996**, *29*, 268−276.
(11) *Field Flow Fractionation Handbook*; Schimpf, M. E., Caldwell, K., Giddings, J. C., Eds.; Wiley-Interscience: New York, 2000.
(12) Williams, S. K. R.; Lee, D. *J. Sep. Sci.* **2006**, *29*, 1720−1732.
(13) Picton, L.; Bataille, I.; Muller, G. *Carbohydr. Polym.* **2000**, *42*, 23−31.
(14) Andersson, M.; Wittgren, B.; Schagerlôf, H.; Momcilovic, D; Wahlund, K. G. *Biomacromolecules* **2004**, *5*, 97−105.
(15) Roger, P.; Baud, B.; Colonna, P. *J. Chromatogr., A* **2001**, *917*, 179−185.

(16) You, S.; Stevenson, S. G.; Izydorczyk, M. S.; Preston, K. R. *Cereal Chem.* **2002**, *79*, 624−630.
(17) Van Bruijnsvoort, M.; Wahlund, K. G.; Nilsson, G.; Kok, W. Th. *J. Chromatogr., A* **2001**, *925*, 171−182.
(18) Wittgren, B.; Wahlund, K. G.; Andersson, M.; Arfvidsson, C. *Int. J. Polym. Anal. Charact.* **2002**, *7*, 19−40.
(19) Lee, S.; Nilsson, P. O.; Nilsson, G. S.; Wahlund, K. G. *J. Chromatogr., A* **2003**, *1011*, 111−123.
(20) Modig, G.; Nilsson, P. O.; Wahlund, K. G. *Starch/Staerke* **2006**, *58*, 55−65.
(21) Botana, A. M.; Ratanathanawongs, S. K.; Giddings, J. C. *J. Microcolumn Sep.* **1995**, *7*, 395−402.
(22) Yu, L.-P.; Rollings, J. E. *J. Appl. Polym. Sci.* **1987**, *33*, 1909−1921.
(23) Zimm, B. H.; Stockmayer, W. H. *J. Chem. Phys.* **1949**, *17*, 1301−1314.
(24) Galinsky, G.; Burchard, W. *Macromolecules* **1997**, *30*, 4445−4453.
(25) Galinsky, G.; Burchard, W. *Macromolecules* **1995**, *28*, 2363−2370.
(26) Aberle, A. T.; Burchard, W.; Vorweg, W.; Radosta, S. *Starch/Stärke* **1994**, *46*, 329−335.
(27) French, D. *J. Jpn. Soc. Starch Sci.* **1972**, *19*, 8−25.
(28) Robin, J. P.; Mercier, C.; Charbonnière, R.; Guilbot, A. *Cereal Chem.* **1974**, *51*, 389−406.
(29) Manners, D. J. *Carbohydr. Polym.* **1989**, *11*, 87−112.
(30) Gérard, C.; Planchot, V.; Colonna, P.; Bertoft, E. *Carbohydr. Res.* **2000**, *326*, 130−144.
(31) Bertoft, E. *Carbohydr. Res.* **1989**, *189*, 181−193.
(32) Bertoft, E.; Spoof, L. *Carbohydr. Res.* **1989**, *189*, 169−180.
(33) Bertoft, E.; Zhu, Q.; Andtfolk, H.; Jungner, M. *Carbohydr. Polym.* **1999**, *38*, 349−359.
(34) Zhu, Q.; Bertoft, E. *Carbohydr. Res.* **1996**, *288*, 155−174.
(35) Yao, Y.; Thompson, D. B.; Guiltiman, M. J. *Plant Physiol.* **2004**, *136*, 3515−3523.
(36) Hizukuri, S. *Carbohydr. Res.* **1986**, *147*, 342−347.
(37) Thompson, D. B. *Carbohydr. Polym.* **2000**, *43*, 223−239.
(38) Castro, J. V.; Dumas, C; Chiou, H.; Fitzgerld, M. A.; Gilbert, R. G. *Biomacromolecules* **2005**, *6*, 2248−2259.
(39) Nilsson, G. S.; Bergquist, K.-E.; Nilsson, U.; Gorton, L. *Starch/Stärke* **1996**, *48*, 352−357.
(40) Burchard, W. *Macromolecules* **1972**, *5*, 604−610.
(41) Ioan, C. E.; Aberle, T.; Burchard, W. *Macromolecules* **1999**, *32*, 7444−7453.
(42) Calder, P. C. *Int. J. Biochem.* **1991**, *23*, 1335−1352.
(43) Planchot, V.; Colonna, P. and Saulnier, L. In *Guide Pratique d'Analyses dans les Industries des Céréales*; Godon, B., Loisel, W., Eds.; Lavoisier: Paris, France, 1997; pp 341−398.
(44) Wyatt, P. J. In *Laser Light Scattering in Biochemistry*; Harding, S. E., Satelle, D. B., Bloomfield, V. A., Eds.; Royal Society of Chemistry: Cambridge, U. K., 1992; pp 35−58.
(45) Hanselmann, R.; Burchard, W.; Ehrat, M.; Widmer, H. M. *Macromolecules* **1996**, *29*, 3277−3282.
(46) Flory, P. J. *Principles of Polymer Chemistry*; Cornell University Press: Ithaca, NY, 1953.
(47) Erlander, S.; French, D. *J. Polym. Sci.* **1956**, *20*, 7−28.
(48) Burchard, W. *Macromolecules*, **1977**, *10*, 919−927.
(49) Burchard, W. *Adv. Polym. Sci.* **1983**, *48*, 1−124.
(50) Burchard, W. *Adv. Polym. Sci.* **1999**, *143*, 113−194.
(51) Stauffer, D. *Phys. Rep.* **1979**, *54*, 1−74.
(52) Bello-Pérez, L. A.; Roger, P.; Colonna, P.; Paredez-Lopez, O. *Carbohydr. Pol.* **1998**, *37*, 383−394.
(53) Hizukuri, S. *Carbohydr. Res.* **1985**, *141*, 295−306.
(54) Shi, Y.-C.;Seib, P. A. *Carbohydr. Res.* **1992**, *227*, 131−135.
(55) Caldwell, R. A.; Matheson, N. K. *Carbohydr. Polym.* **2003**, *54*, 201−213.
(56) Yun, S.-H.; Matheson, N. K. *Carbohydr. Res.* **1993**, *243*, 307−321.
(57) Burchard, W. *Macromolecules* **2004**, *37*, 3841−3849.
(58) Arfvidsson, C.; Wahlund, K. G. *J. Chromatogr., A* **2003**, *1011*, 99−109.
(59) Caldwell, K. D., Brimhall, S. L., Gao, Y., Giddings, J. C. *J. Appl. Polym. Sci.* **1988**, *36*, 703−719.
(60) Colfen, H.; Antonietti, M. *Adv. Polym. Sci.* **2000**, *150*, 67−187.

BM070024Z